European volcanological supersite in Iceland: a monitoring system and network for the future

Report

D6.6 - Methodology and strategy for interpretation of multidisciplinary 'eruption phase' data in FUTUREVOLC

Work Package:	*Imminent eruptive activity, eruption onset and early warning*
Work Package number:	*6*
Deliverable:	*Methodology and strategy for interpretation of multidisciplinary 'eruption phase' data in FUTUREVOLC*
Deliverable number:	*6.6*
Type of Activity:	*RTD*
Responsible activity leader:	*Kristin Vogfjord*
Responsible participant:	*University College Dublin*
Authors:	*Maurizio Ripepe, Eva Eibl, Christopher Bean, Kristin Vogfjord*

Type of Deliverable:	*Report*	*[X]*	*Demonstrator*	*[ ]*
	Prototype	*[ ]*	*Other*	*[ ]*
Dissemination level:	*Public*	*[X]*	*Restricted Designated Group*	*[ ]*
	Prog. Participants (FP7)	*[ ]*	*Confidential (consortium)*	*[ ]*

Seventh Framework Programme
EC project number: 308377

Summary

Here we demonstrate efforts at the joint interpretation of multi-disciplinary data streams from both eruptive and flooding environments. For the eruptive case we consider the relationships between RMS seismic signals, acoustic signals and effusive rate. During the eruption there is a good correlation between RMS seismic amplitude and acoustic pressure signals, suggesting that the seismic signals are related to eruptive product output rates. There is also a good correlation between the acoustic amplitude and the effusive rate measured by satellite, which shows how the acoustic pressure decays with time following a similar decay in the effusion rate. In fact the acoustic signals decays in correlation with effusion rate and ends with the termination of the eruption, offering a potential remote real-time methods for eruption monitoring.
In contrast during a flooding there is no correlation between the seismic signals and the acoustic signals. However seismic tremor correlated well with GPS and river gauge data demonstrating that, whilst acoustic signals hold little information about flooding events, seismic tremor can be used to monitor sub-glacial floods.

Introduction

The quantitative interpretation of multi-disciplinary data streams in heterogeneous volcanic environments is a very challenging problem. Qualitatively the various data streams can be visually compared for related trends. However full quantitative analysis requires a formalised 'joint inversion'. This has its own drawbacks as, for example, it is difficult to know *a priori*, how to weight the individual data streams. A practical 'middle ground' is the cross-correlation of the various datasets or the monitoring of cumulative trends in data. Over the lifetime of the FutureVolc project, there were two major events during which multiple data streams were obtained (i) Holuhraun eruption in 2014 (ii) The flooding event from western Vatnajökull in 2015. Here we show examples of multi-disciplinary data for both of these events and efforts to jointly interpret them using correlation analysis.

Eruption Joint interpretation: Seismo-Acoustic and Acoustic-effusion rate coupling

Migration of magma, and/or magmatic fluids, inside the volcanic edifice along dykes, conduit or magma chambers generate seismic signals. These signals are difficult to discriminate from seismic signals produced by magma/lava flowing outside the volcanic crater during an eruption. This dilemma for volcano seismology has a strong impact on the use of seismic monitoring to deliver reliable and timely warning of imminent eruptive activity. One way to address this problem is to compare seismic signals to other data streams - making that comparison on the basis of a conceptual model of the underlying processes. We might consider that we expect magma moving inside the volcanic 'edifice' to have little or no coupling to the atmosphere whereas we expect the outflow of the magmatic fluids during an eruption to show strong atmospheric coupling.

Here we use this expected difference in coupling with the ground and with the atmosphere to address the source question outlined above.

Coupling seismic and acoustic wavefield

The algorithm developed uses infrasonic and seismic signals recorded at co-located sites and is based on the cross-correlation analysis of the seismo-acoustic waveforms. The algorithm makes use of the cross-correlation function between the vertical ground motion and the infrasound. If the vertical ground motion is generated by the ground

coupling of infrasonic waves, the correlation function will be delayed by a quarter of a cycle relative to the pressure wave (Ichihara et al., 2011). This particular pattern allows the detection of seismic signals linked to sources that are well coupled with the atmosphere. Also the correlation pattern will change when the relative amplitude of infrasound and seismic wave changes, as expected during changes in eruptive activity. This technique is also very effective in reducing the effect of the wind noise. In fact, contribution of wind noise to the correlation function is suppressed by separating the microphone and the seismometer by several meters because the correlation length of wind noise is much shorter than wavelengths of infrasound.

The algorithm has been successfully tested on seismic signals recorded by the station specifically collocated together with a 4-element small aperture infrasonic array during the 2014 Holuhraun eruption (Figure 6.6.1).

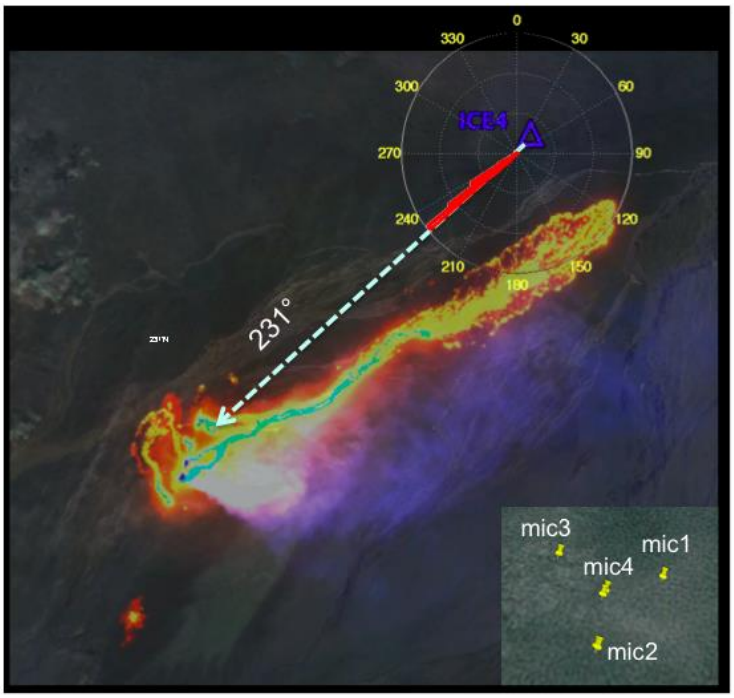

Figure 6.6.1 Location of the small-aperture infrasonic array and the co-located seismic station at 11 km from the effusive Holuhraun vent. The white arrow indicates the backazimuth of the infrasonic wavefield detected by the array, which coincides with the position of the effusive vent.

Seismic and infrasonic signals have been filtered in the 0.5 – 4 Hz frequency band and then cross-correlation has been applied to 4-s long time windows with no overlap. During the eruption the algorithm shows a clear correlation coefficient with positive and negative peak around the zero indicating the strong contribution of an infrasonic source to the tremor (Figure 6.6.2). Instead on February 28th, when the eruption ceased, seismic and infrasound do not show any correlation indicating that the acoustic source is no longer present in the seismic wavefield (Figure 6.6.3). This technique could be easily applied as monitoring tool to retrive information about volcanic activity more effectively than infrasound or seismic signals alone, because it reflects both features of incident infrasonic and seismic waves. Therefore, a graphical presentation of temporal variation in the cross-correlation function enables one to see qualitative changes of eruptive activity at a glance.

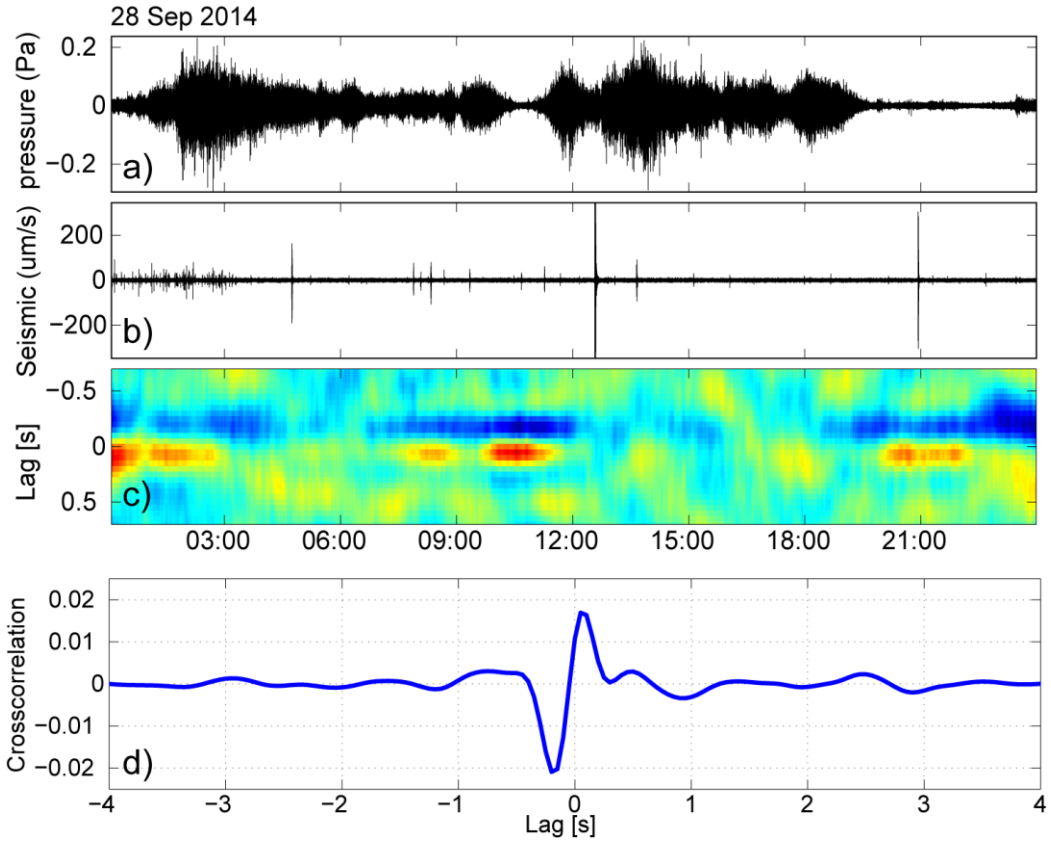

Figure 6.6.2. Example of infrasonic (a) and seismic (b) interaction recorded at the same site (Figure 6.6.1) on the 28th Sep. 2014. Data filtered in the 0.4-5 Hz have been cross-correlated (c) following the procedure described by Ichihara et al., 2012 in a 4-s time window and then averaged over one-hour intervals (c). The correlation map show a clear correlation indicating a strong seismic air-coupled effect. (d) correlation is then stacked to calculate the average correlation function for the whole day.

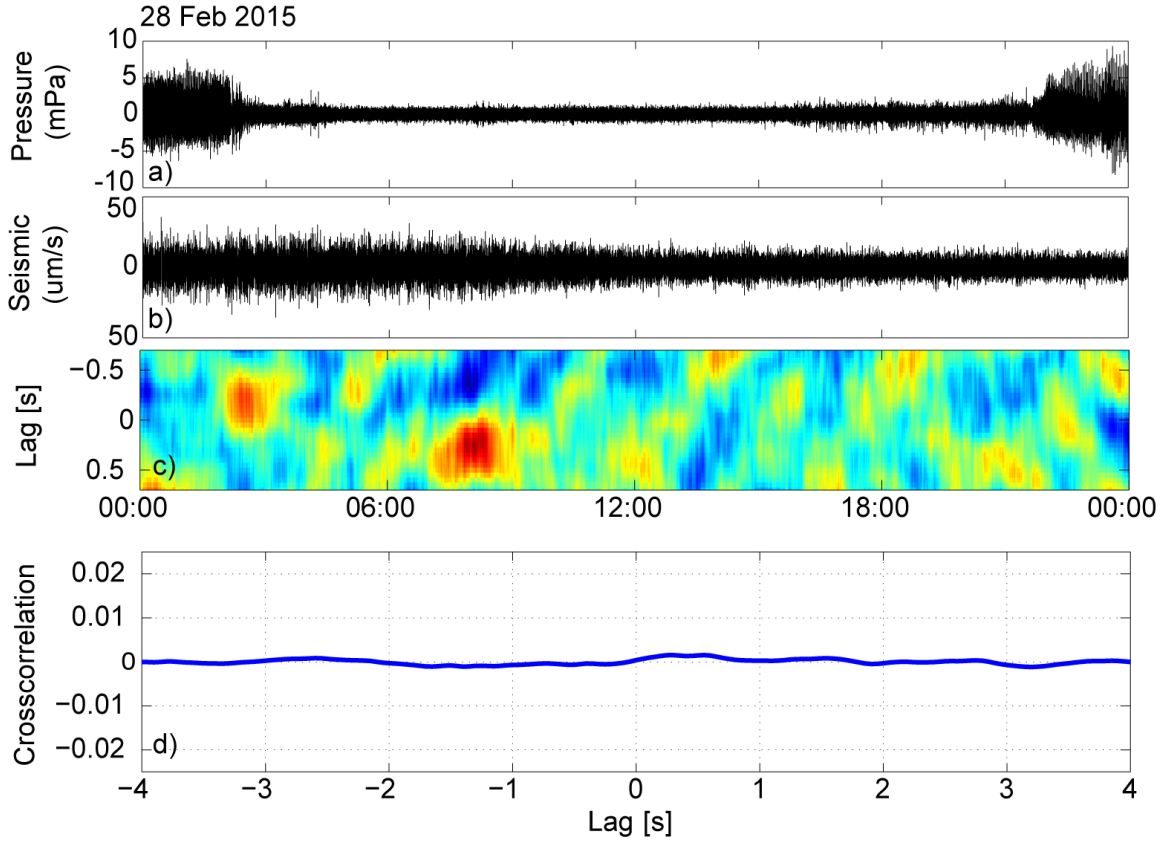

Figure 6.6.3. Example of infrasonic (a) and seismic (b) interaction recorded at the same site as for Figure 6.6.2 on the 28th February 2015, after the eruption. Data have been processed following the same procedure as Figure 6.6.2 but in this case the correlation map (c) does not show a correlation indicating that no infrasound is transmitted to the ground. Correlation map is then stacked to calculate the average correlation function (d) for the whole day and also in this case it is evident how there is no infrasonic energy transmitted to the ground, which indicates the absence of an explosive source well coupled with the atmosphere.

Integrating Acoustic wavefield with Effusion rate

During the Holuhraun eruption about 1.8 km^3 of lava was erupted through a dike 45 km long, that connected the eruptive site (Figure 6.6.1) to the plumbing system of Bárðarbunga volcano. Systematic satellite measurements of the heat radiated by the lava field based on MODIS (Moderate Resolution Imaging Spectroradiometer) data been used to decode the effusive trend and to quantify lava discharge rates during the Holuhraun eruption in near-real-time (Tarquini et al., 2015). Effusive trend shows (Figure 6.6.4) that lava flux peaked at ~350 m^3 s^{-1} at the beginning of the eruption (early September 2014), and slowed down in the following months, reducing to ~250 m^3 s^{-1} in October and to ~150 m^3 s^{-1} in November 2014. Conversely, since early December 2014 the main lava channel(s) started to crust over and the flow field thickened through overlapping of insulated flows. At this time the effusion rates declined gently to ~100 m^3 s^{-1} reducing to ~50 m^3 s^{-1} at the end of January 2015 (Figure 6.6.4) and on February 26th 2015, the eruption was declared over.

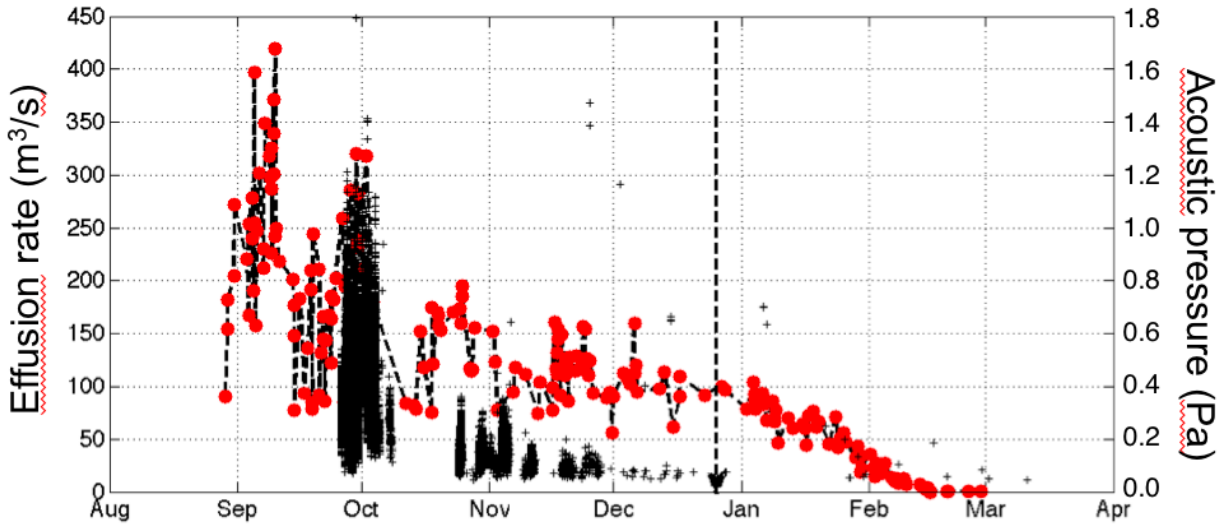

Figure 6.6.4. Effusion rate (red dots) calculated using thermal radiance measured by MODIS is compared to the infrasonic detections (black crosses) located by the array in the same direction as the Holuhraun effusive fissure (Figure 6.6.1). Amplitude of the infrasonic pressure decreases following the same trend as the effusive rate indicating the control of the effusive rate on the spectacular lava fountaining activity observed at the Baugur crater. Note that infrasound in not detected after the end of December (black dashed arrow), which coincides with the onset of the effusive rate decay.

The infrasonic array ICE4 deployed at the end of September is used to calculate the wave propagation back-azimuth, apparent velocity and time residual using a multi-channel correlation algorithm. The analysis shows a persistent signal coming from 231°N consistent with the relative position of the effusive vent (Figure 6.6.1). Infrasound indicates that the spectacular *lava fountaining* activity at the effusive Baugur fissure vent was the source of sound recorded at 11 km distance with amplitudes as weak as <1.2 Pa. This gives a reduced infrasonic amplitude at 1 km of only ~11 Pa which is very small if compared to 800 Pa maximum reduced amplitude recorded during the second explosive phase of the 2010 Eyjafjallajokull eruption. Besides, the weak amplitude recorded at the ICE4 array explains why this spectacular activity was not detected by the other arrays located at >100 km away. The weak pressure amplitude could be a consequence of the large area covered by the Baugur vent or it can indicate that this explosive process was in reality driven by a gas-poor magma or better by a magma which was reaching the vent almost completely degassed.
This scenario seems also confirmed by the correlation between the acoustic amplitude and the effusive rate measured by satellite, which shows how the acoustic pressure decays with time following a similar decay in the effusion rate.
It is worth noting that the array is not detecting a persistent activity after the second half of December 2015 (dashed arrow in Figure 6.6.4), as is also confirmed by on-site observations. The end of infrasonic activity coincides with the onset of the decreasing trend in the effusive rate below 100 m^3/s. The correlation between infrasonic detections and effusive rate points also to a lava fountaining dynamics of the Baugur lava lake driven by the effusive flow rate rather than by the magma gas overpressure. This latter correlation points to a scenario where the magma reaches the effusive vent already partially degassed or with the gas in equilibrium conditions.

The results above show the effectiveness of structured (here correlation analysis) interpretation of multi-disciplinary data sets.

Integrating Seismic wavefield with Effusion rate

The relationship between the seismic and acoustics wavefields is quantified above, in the previous section. Also the acoustic wavefield is compared to the effusion rate. Here the seismic wavefield can also be directly compared to the effusion rate.

In figure 6.6.5 we show a comparison of Root Median Square (RMeS) of seismic tremor during the 6 months of eruption with pressure detected at an infrasound array, three flux rates derived using satellites, the added area or the total area covered, magma discharge rate and SO_2 flux. Tremor amplitude and flux rates correlate well in broad scale trend.

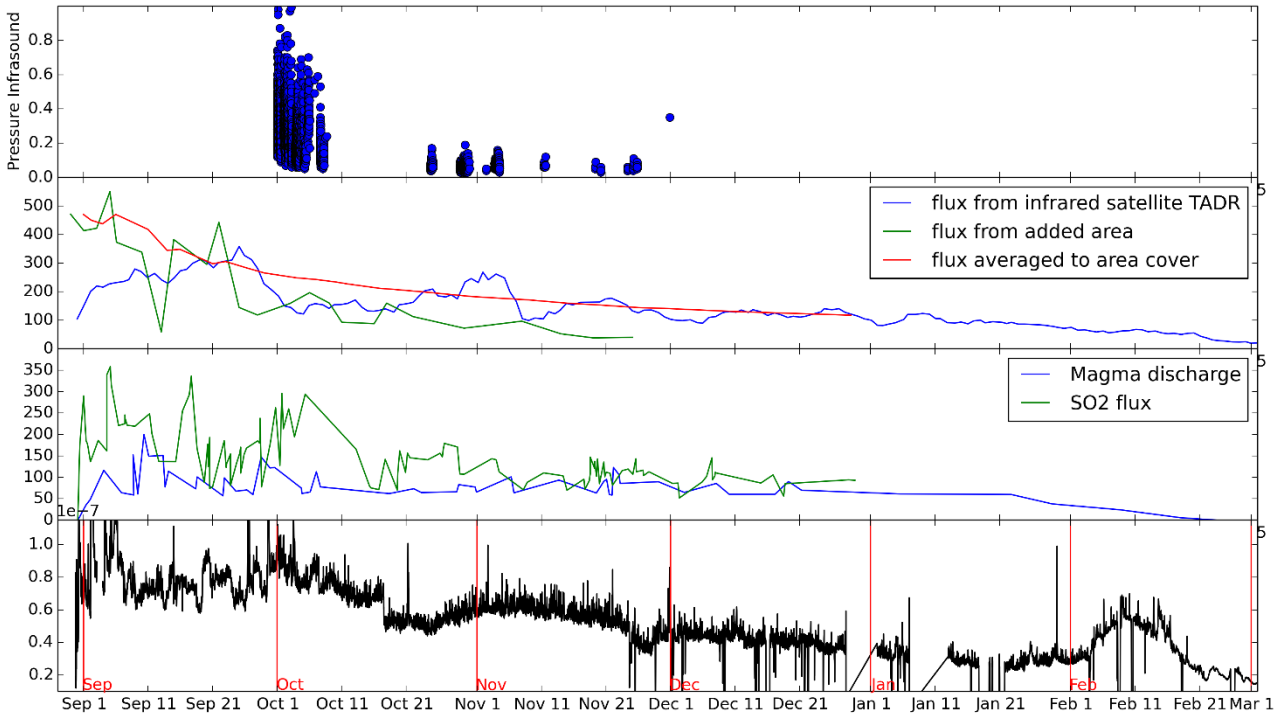

Figure 6.6.5: Comparison of a variety of parameters during the eruption. From top to bottom: pressure detected by an infrasound array; Flux rate derived from an infrared satellite TADR, from the added area and averaged over the area covered; Magma discharge and SO2 flux rate; and RMeS of the tremor at UR array.

Note from D6.3 on Seismic, InSar, GSP, Cauldron Observations and full wavefield numerical simulation joint interpretations.

Data from UR seismic array was combined with satellite, InSar, GPS, observations of cauldrons, geodetic measurements, full wavefield simulations and single seismic stations. By integrating these datasets we have recently determined that an 18 h long tremor pulse on September 3rd 2014 was not due to a flood but was due to upward dyke propagation. Attempts to determine if this tremor pulse was related to a flood or magma failed in 2014 as the array processing was not yet sufficiently tested & integrated with other datasets. A paper on this topic has recently been submitted (Eibl et al 2016) - see also D6.3.

<u>Flooding joint interpretation</u>: Seismo-GPS-River Gauge comparisons

Floods from Grímsvötn down Skeiðarárjökull and the Skaftá cauldrons down Skaftárjökull are common. The latter cauldrons drain about every two years. In order to improve the early warning for these floods we installed two arrays southwest of Vatnajökull glacier around Skaftá river, a streaming GPS instrument in the eastern cauldron and two GPS stations on top of the flood path on Skaftárjökull. This dataset was completed with data from river gauges and an osmotic sampler in Skaftá. Additionally there was an infrasound array in Kirkubaej arkloestur.
Figure 6.6.6 shows the location of the arrays with respect to the GPS stations.

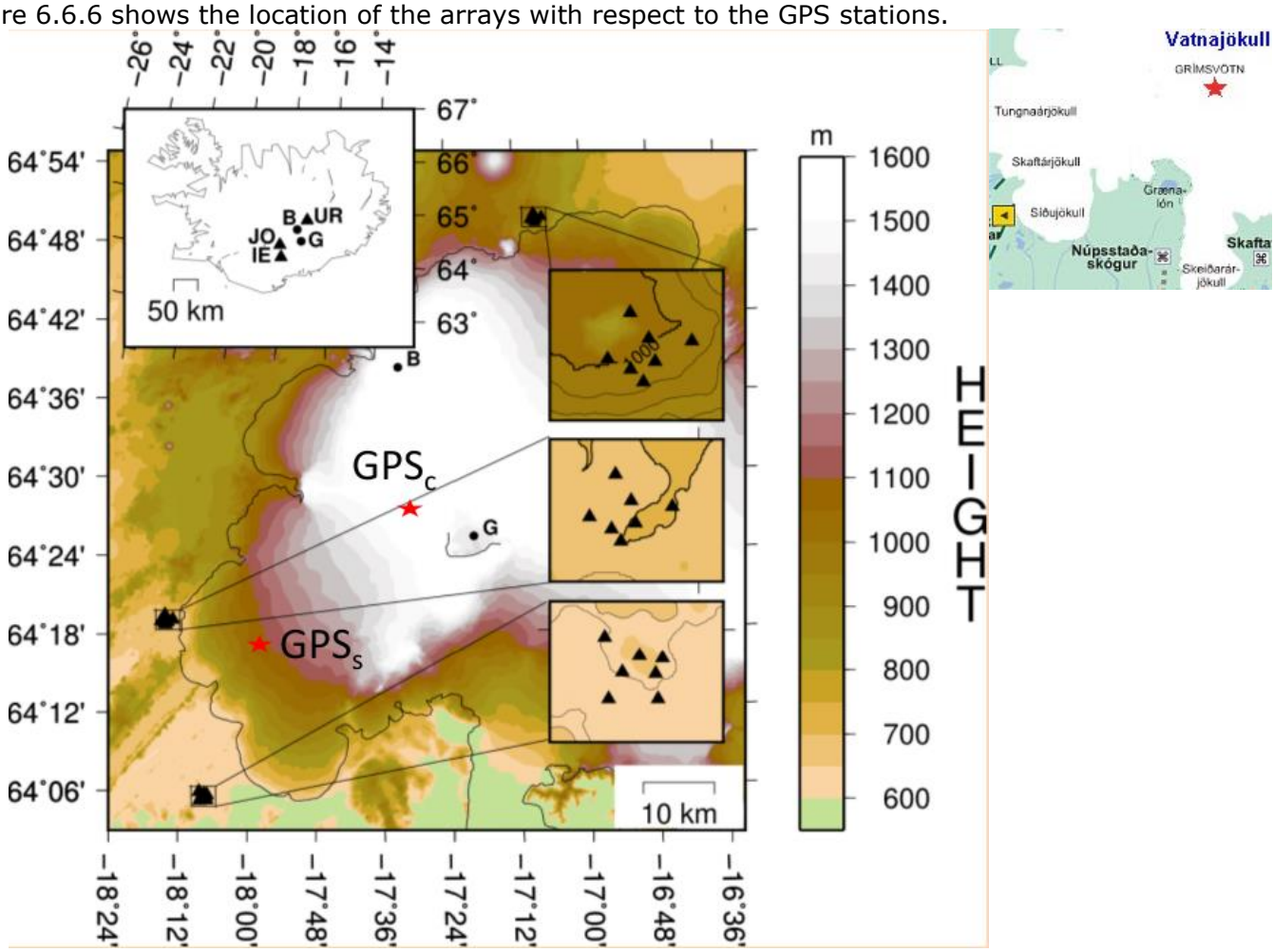

Figure 6.6.6: (left) Geometry and location of three 7-instrument arrays near Laki (IE), Jökulheimar (JO) and Urðarháls (UR), red stars mark GPSc and GPSs. Bardarbunga (B) and Grímsvötn (G) are marked with black dots. (right) Zoom in around Grímsvötn (red star)

The river gauges, arrays and GPSs monitored the two cauldrons and the caldera over almost the last two years. In that time period two small floods from the western cauldron, a small flood from Grímsvötn and a large flood from the eastern cauldron were recorded. As the river gauges will detect a flood with a delay of a few days, our main focus was on the arrays and GPS instruments. In periods with seismic tremor a direction from which the tremor was coming (backazimuth) could be obtained, and one of these pulses was located at Hofsjökull rather than the Skaftá cauldrons.
We combined the three datasets mentioned above in order to estimate the speed of a flood (i.e. by combining the GPS in the cauldron and a river gauge or the speed of migration of the tremor source). We can also comment on the type of activity by the

lack, presence or movement of the tremor source. In October 2015 the eastern cauldron finally drained after 5 years. The flood was bigger than usual, with 2094 m³/s of discharge. The GPS instrument in the cauldron gave an unprecedented early warning (see fig 6.6.7)

Figure 6.6.7 shows the seismic tremor trace, in conjunction with the tremor source direction obtained from JO array and the GPS traces of GPSs (on top of the flood path) and GPSc (in the cauldron). The second GPS instrument on the flood path was lost during the flood. On September 27th the GPS in the cauldron started to drop in elevation. At this time the water started to slowly drain. The first tremor (90 deg from JO) is visible late on September 30th well down the flood path shortly after the flood had started to lift GPSs. In the early hours of October 1st the tremor shows that it had reached the edge of the glacier (figure 6.6.7). Which is in accordance with the gauge in Sveinstindur in Skaftá river (figure 6.6.8) where the water started to rise at around 4 am on October 1st. Then GPSc in the cauldron (figure 6.6.7) starts to level out, indicating that the water has largely discharged by late on October 1st. However, tremor bursts start from the direction of the cauldron once GPSc levels out. These are related to hydrothermal boiling or small eruptions that can happen when the pressure in the cauldron suddenly drops.

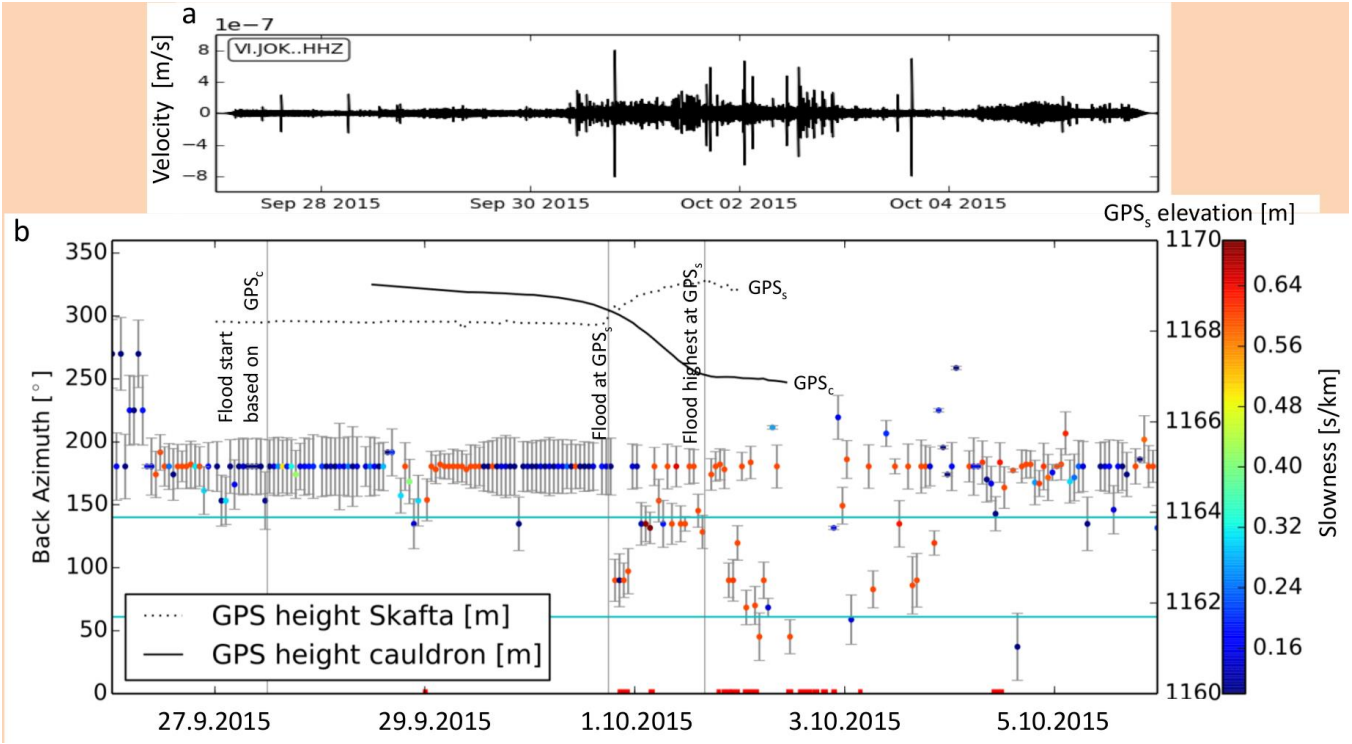

Figure 6.6.7: (a) Seismogram during the flood, filtered 0.9-2.6 Hz. (b) Overview of the predominant back azimuth in one hour long time windows in September and October 2015 for an array analysis performed at JO array in the 0.8-2.4 Hz band. We mark the beginning of the flood (GPSc), the arrival of the flood at GPSs and the highest elevation of GPSs during the flood with grey vertical lines. The blue lines indicate the expected back azimuths of the source of Skaftá river and the eastern cauldron. Points are coloured according to slowness. The red lines mark visually observed tremor, the black curves the elevation of the GPS in the Eastern cauldron GPSc and Skaftárjökull GPSs. GPS data provided by Jóhannesson et al, 2015.

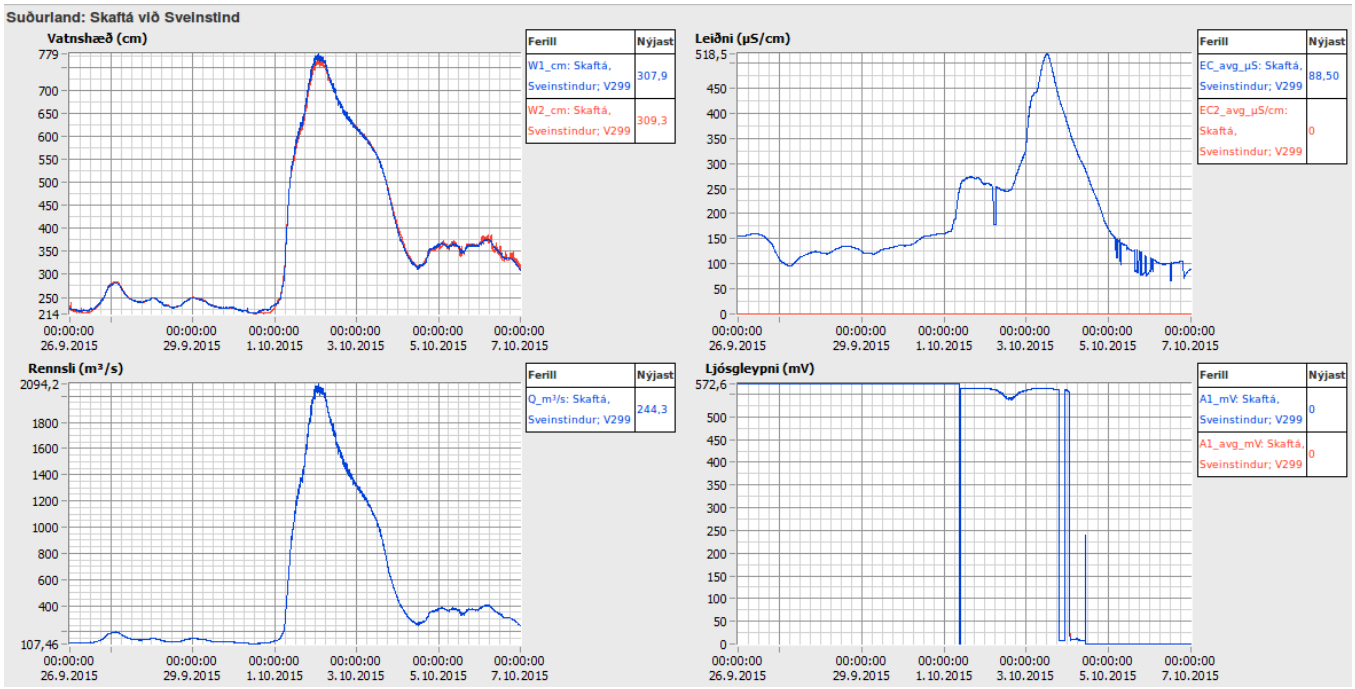

Figure 6.6.8: During the Skaftá flood gauges in various rivers (here station Sveinstindur in Skaftá river) detected peaks in (top left) water elevation, (top right) conductivity and (bottom left) discharge.

A second promising event is a flood from the Grímsvötn caldera down Skeidararjökull in May 2015 (figure 6.6.9). The arrays IE and JO recorded the flood and a change in back azimuth. We can use this in order to deduce a speed and will combine it with data from the GPS station inside the caldera and water level measurements south of Skeidararjökull. This work is still in progress but initial array results are excellent, giving a clear indication of the flood origins of the tremor from Grímsvötn.

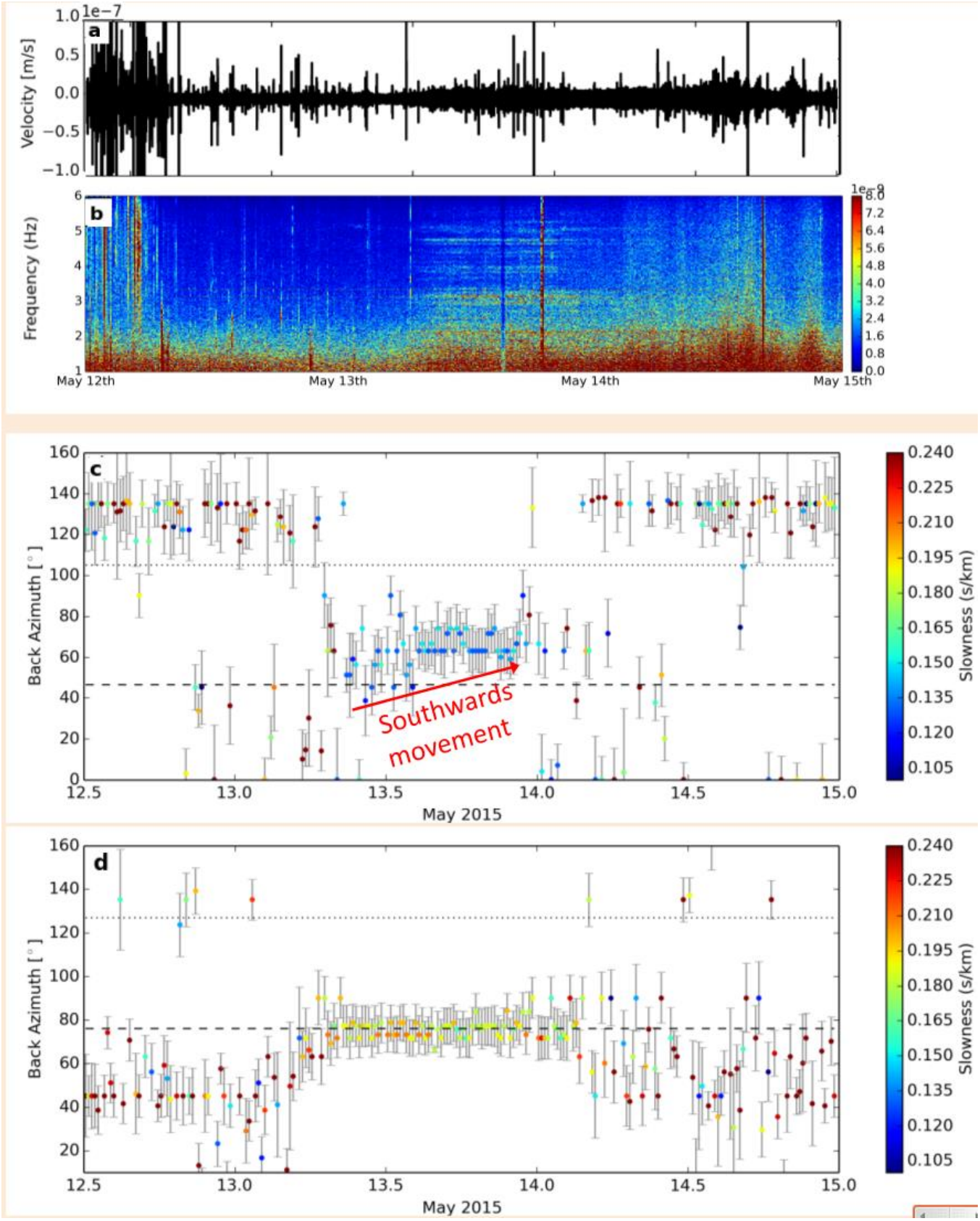

Figure 6.6.9: (a) Seismogram at JO array filtered 1-6 Hz from May 12th to May 15th , 2015. (b) Spectrogram. (c) Back azimuth at IE array coloured according to slowness when filtered to 2.4-4.2 Hz. Horizontal lines mark the back azimuth expected for signals from the Grimsvötn caldera (dashed) and at the outlet of Skeidararjökull (dotted). (d) Same as c but for JO array.

Recap note from D6.4 on Geodetic and Seismic data

Deliverable 6.4 demonstrates how high-rate geodetic and seismic data can be integrated in near-real-time for volcanic monitoring purposes. The work takes advantage of the latest developments in data streaming and graphical visualisation. It addresses a fundamental requirement to minimise the time-delay between raw data collection and the availability of useable, multidisciplinary monitoring results. Data are processed into easily understandable visual displays, enabling monitoring scientists and hazard managers to evaluate ongoing hazards in near-real-time. The freely available R programming language was used to process and visualise various types of geophysical data. A processing environment was developed to minimise the time-delay between data collection and the display of useable results. Two combined online displays were developed, one for continuous monitoring of the Hekla volcano and the other for following caldera subsidence at the Bárðarbunga volcano between September 2014 and February 2015. The results show how automated, rapidly available data-plots can be used to follow escalating levels of volcanic unrest in near-real-time.

Conclusion

This deliverable on multi-disciplinary data analysis demonstrate the power of formally quantifying the relationships between different data streams in both eruptive and flooding environments. The quantification also allows us to estimate the power of individual methods in cases where they will, in the future, be the only data streams available. Key findings are: (i) acoustic data can be used as a proxy for eruption effusive rate and offers a potentially powerful tool for remotely monitoring an eruption at very high temporal resolution (ii) seismic tremor and GPS are both powerful tools for monitoring (sub-glacial) floods and in particular seismic array data can be used to track flood evolution.

References

Björnsson, H., 1977, The cause of Jökulhlaups in the Skafta River, Vatnajökull. Jökull 27 (71)

Einarsson, B., Magnússon, E., Roberts, M. J., Pálsson, F., Thorsteinsson,T, Jóhannesson, T., (in press) A spectrum of jökulhlaup dynamics revealed by GPS measurements of glacier surface motion, Annals of Glaciology

Roberts, M. J., Palsson,F., Gudmundsson, M. T., Bjornsson, H., Tweed, F. S., (2005). Ice–water interactions during floods from Grænalon glacier-dammed lake, Iceland, Annals of Glaciology 40

Ichihara, M., Takeo, M. and Yokoo, A. (2011). Monitoring volcanic activity using correlation patterns between infrasound and ground motion, *Geophysical Research Letters*,doi:10.1029/2011GL050542

Johannesson, T., (2002). The initiation of the 1996 jôkulhlaup from Lake Grimsvôtn, Vatnajôkull, Iceland, Proceedings of a symposium held at Reykjavik. Iceland. IAHS Publ. no. 271

Jóhannesson, T., B. Einarsson, B.G. Ófeigsson, M.J. Roberts, Þ. Þorsteinsson and K. Vogfjörð (2015). A record jökulhlaup in River Skaftá from the Eastern Skaftá Cauldron. Abstract, International Glaciological Society, Nordic Branch Meeting, 29 - 31 October.

Tarquini, S., Vitturi, M., Jensen, E., Barsotti, S., Pedersen, G., and Coppola, D. (2015). Simulating the lava flor formed during the 2014-2015 Holuhraun eruption (volcanic system, Iceland) by using the new F-L probabilistic code, *Geophysical Research Abstracts*, Vol 17, EGU2015-11851.